RAY TRACING FOR MODELING OF SMALL FOOTPRINT AIRBORNE LASER SCANNING RETURNS

Felix Morsdorf[a], Othmar Frey[a], Benjamin Koetz[b], Erich Meier[a]

a) Remote Sensing Laboratories, Department of Geography,University of Zurich
email:felix.morsdorf, othmar.frey, erich meier@geo.uzh.ch
b) ESA-ESRIN, Exploitation & Services Division, Project Section
email:Benjamin.Koetz@esa.int

Commission III, WG 3

ABSTRACT:

Airborne Laser Scanning (ALS) has been established as a valuable tool for the estimation of biophysical canopy variables, such as tree height and vegetation density. However, up to now most approaches are built upon empirical stand based methods for linking ALS data with the relevant canopy properties estimated by field work. These empirical methods mostly comprise regression models, where effects of site conditions and sensor configurations are contained in the models. Thus, these models are only valid for a specific study, which renders inter-comparison of different approaches difficult. Physically based approaches exist e.g. for the estimation of tree height and tree location, however systematic underestimation depending upon sampling and vegetation type remains an issue. Using a radiative transfer model that builds on the foundation of the Open-Source ray tracer povray we are simulating return signals for two ALS system settings (footprint size and laser wavelength). The tree crowns are represented by fractal models (L-systems), which explicitly resolve the position and orientation of single leafs. The model is validated using ALS data from an experiment with geometric reference targets. We were able to reproduce the effects of target size and target reflectance that were found in the real data with our modeling approach. A sensitivity study was carried out in order to determine the effect of properties such as beam divergence (0.5, 1, and 2 mrad), canopy reflectance (laser wavelength, 1064 and 1560 nm) on the ALS return statistics. Using the two laser wavelengths above, we were able to show that the laser wavelength will not significantly influence discrete return statistics in our model. It was found that first echo return statistics only differ significantly if the footprint size was altered by a factor of 4. Last return distributions were significantly different for all three modelled footprint sizes, and we were able to reproduce the effect of an increased number of ground returns for large footprint sizes. These forward simulations are a first step in the direction of physically based derivation of biophysical ALS data products and could improve the accuracy of the derived parameters by establishing correction terms.

1 INTRODUCTION

In recent years, Airborne Laser Scanning (ALS) was established as a valuable tool for the horizontal and vertical characterization of the vegetation canopy. A number of studies prove ALS to be capable of deriving canopy height, be it for stands [Lefsky et al., 1999; Means et al., 2000; Næsset and Bjerknes, 2001] or single trees [Hyyppä et al., 2001; Persson et al., 2002; Morsdorf et al., 2004]. Furthermore, ALS was used to derive measures of vegetation density such as fractional cover (fCover) and/or leaf area index (LAI) [Harding et al., 2001; Lovell et al., 2003; Morsdorf et al., 2006b]. These approaches can be divided into two classes, empirical and physical methods. Tree height and crown width are mostly directly computed from either a gridded canopy height model (CHM) or the point cloud itself, making it a physical approach as e.g. the tree segmentation algorithm proposed by Morsdorf et al. [2004] (Figure 1). On the other hand approaches deriving fCover and LAI most often use regression models to link ground measurements with laser predictor variables, making it an empirical method.

These products comprise site and instrument specific properties, such as different sensor types, vegetation types and viewing geometry. This makes the comparison of results from different sites and sensor configurations hard, if not impossible. For instance, it is expected that laser wavelength and footprint size have an influence on the magnitude of these parameters. Some research has already been pointing in this direction. A study of Yu et al. [2004] showed that tree height underestimation was larger for higher flying heights (and consequently larger footprint size), as well as that fewer trees were detected the higher the flying altitude was. These results are backed (among others, e.g. Gaveau
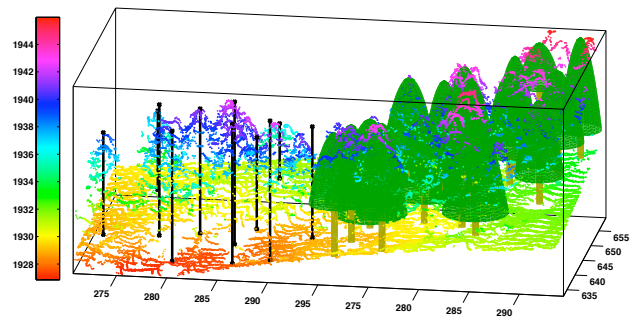

Figure 1: Illustration of physically based tree segmentation algorithm based on cluster analysis of raw data. For details see Morsdorf et al. [2004].

and Hill [2003]) by Morsdorf et al. [2006a], who showed that tree height underestimation in a mountain pine forest would increase by about 30 cm when changing the flight altitude from 500 m AGL to 900 m AGL. However, it remains unclear how much the lower sampling density or the larger footprint size contribute to this increase in tree height underestimation. As it is very hard to separate these effects in empirical studies such as the one of Morsdorf et al. [2006a], one has to find alternative solutions in retrieving information on the magnitude of these effects on biophysical parameter estimation. Modelling of laser returns using geometrical-optical models might help here. Such approaches have been carried out for large footprint data, where the tree crowns where represented by cones filled with a turbid medium [Sun and Ranson, 2000; Ni-Meister et al., 2001; Koetz

et al., 2006], but so far not for small-footprint ALS data. For small footprint data, the tree models need to be more complex and should explicitly resolve the tree structure at the leaf level, whereas for modeling large footprint data it was sufficient to spatially resolve the canopy at the crown level [Sun and Ranson, 2000]. In recent years, fractal models of tree geometry have been developed which resolve the tree geometry at the leaf level. These models are used for ecological studies as well as for producing realistically looking computer rendered images of vegetation. Thus, our objective is to use such fractal models of tree geometry and a commonly used ray-tracer to study the effect of footprint size and laser wavelength on ALS return distributions, which are the basis for most ALS based biophysical vegetation products. This approach should enable one to simulate individually the effects of acquisition properties such as incidence angle, point density, terrain slope, laser footprint size, laser wavelength and canopy reflectance on the accuracy of biophysical vegetation data products opposed to real-world scenarios, where all these effects contribute indifferently to differences between ground truth and ALS based estimations of biophysical parameters. A special challenge will be to model the sensor characteristics of the Toposys FALCON II system used for validation. This needs to be done, since we use discrete return data for validation, which is highly susceptible for the methods of echo detection applied by the system provider.

2 METHODS

2.1 Modeling of ALS data

2.1.1 Ray-tracing using povray
Povray[1] is an open-source ray tracing software that is widely used in computer graphics for the visualization of scenes with arbitrary complex geometry. It has as well been used for scientific visualizations [Solenthaler et al., 2007], but so far not for simulating optical devices, except for optical benches. However, we believe that it might be used for the simulation of ALS return signals, since it allows for representing complex geometries as well as differences in object reflectance and transmission. Povray uses backward ray-tracing to infer whether a beam from a light-source is reflected from an object in a scene into the camera. The description of the scene including object, light and camera location and properties, is done using it's own scene description language. A series of commands is written into include files (.inc) and is then parsed by the program. Povray allows for several lights and camera modes, we use a spotlight with a defined beam divergence resembling that of the Toposys instrument. Inside the beam, the energy distribution is not uniform, but of Gaussian shape. According to the system manufacturer, the beam divergence defines the point where the intensity of the beam has fallen off to $1/e$ of its peak (center) energy. The spotlight used in our simulations has been configured accordingly. An orthographic camera is used which is placed directly above the object. The spotlight distance was set to 500 meters, the incidence angle to zero degrees, and for each of the experiments the tree was sampled at a regular grid of 25 cm spacing in both x and y direction, summing up to about 1000 waveforms.

2.1.2 Constructing an ALS return signal
We use a special version of povray, MegaPov[2], which additionally is able to write a depth image from the rendered scene based on the camera position. The resolution of the images was 400 by 400 pixels, resulting in a spatial resolution in the model domain of about 1.5 mm. A combination of the intensity image (povray's primary rendering product) with the depth image will then yield a *return*

---

[1] www.povray.org
[2] http://megapov.inetart.net/

waveform. This is achieved by summing up the pixels P for each range bin $R_i - R_{i+1}$ based on the depth image and multiplying it with the respective mean intensity $\bar{I}$ from the intensity image according to Equation 1. This method is based on the assumption that the leaves are behaving in a lambertian manner.

$$\sigma(R_i, R_{i+1},) = 4 * \sum_{R_i}^{R_{i+1}} P * \bar{I}_{R_i}^{R_{i+1}} \tag{1}$$

This *waveform*, however, represents the range dependent description of the cross-section of the scattering elements in the path of the laser beam rather than the real return waveform of a laser pulse. For obtaining a real waveform, this cross-section still needs to be convoluted with a specific laser pulse [Wagner et al., 2006]. For the Toposys system (see Table 1), this pulse is Gaussian shaped and has a duration of 5 nanoseconds, which equivalents to 1.5 meter in range. Such a pulse is used for the simulations in this study. An illustration of the waveform generation process from the rendered images can be found in Figure 2.

Falcon II Specifications	
Maximum Range	1600 m
Range Resolution	2 cm
Scanning Angle	$\pm 7.15°$
Line-scan Frequency	653 Hz
Pulse Frequency	83 kHz
Laser Wavelength	1560 nm
Number of Fibers	127
Beam Divergence	1 mrad
Pulse length	5 ns

Table 1: Specifications of Falcon II Sensor Platform

2.1.3 Converting the waveform to discrete return data
Since most of the currently available ALS systems are discrete return systems, which do not record the full waveform, but trigger distinct echos in real time from the return signal, we had to simulate this feature as well. For detecting discrete returns from the modelled waveform, we use a Gaussian decomposition as proposed by e.g. Wagner et al. [2006] or Hofton et al. [2000]. This Gaussian decomposition will as well have the advantage of describing the physically meaningful cross-section of the scatterer opposed to plain echo locations in the range dimension. The algorithm we implemented first detects local maxima's from a smoothed version of the return waveform. The location of these maxima's is then used to fit Gaussian functions to the waveform using nonlinear least squares regression. An illustration of the decomposition process can be found in Figure 3. From the reconstructed waveform, adaptive thresholding is used to detect first and last returns as is done for most time-of-flight based LIDAR systems. The height of the threshold is adapted to the maximum intensity of each peak to avoid trigger walk. Using a constant threshold would produce range errors for peaks of different intensity, even if they are at the same location in the range dimension.

2.1.4 Validation
For simulating discrete ALS return data, we faced two challenges. One was the modeling of the return signal (the full waveform) itself and the other was to model the sensor and detector characteristics correctly. For the latter, we were able to use ALS data from an experiment with geometric reference targets on an airstrip close to Zürich. This study was published as Wotruba et al. [2005] and dealt with determining the effects of target size and reflectivity on echo detection and echo separation. We used this data to qualitatively validate our approach by comparing modeled and measured point clouds and studying the effect of target size and reflectance on the echo distribution.
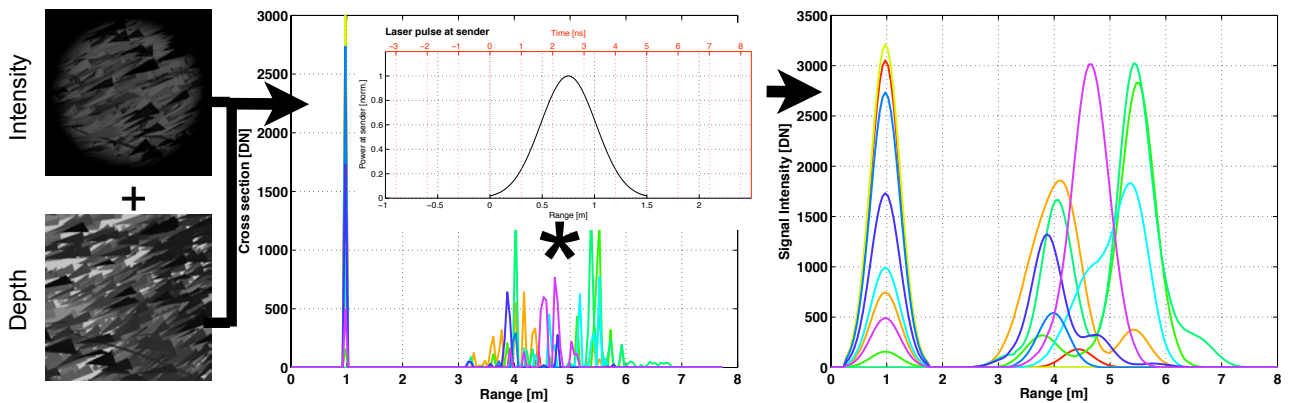
Figure 2: Illustration of waveform generation process based on intensity and depth image and using convolution (denoted by asterisk in middle panel) with a laser pulse of 5 nanoseconds length.
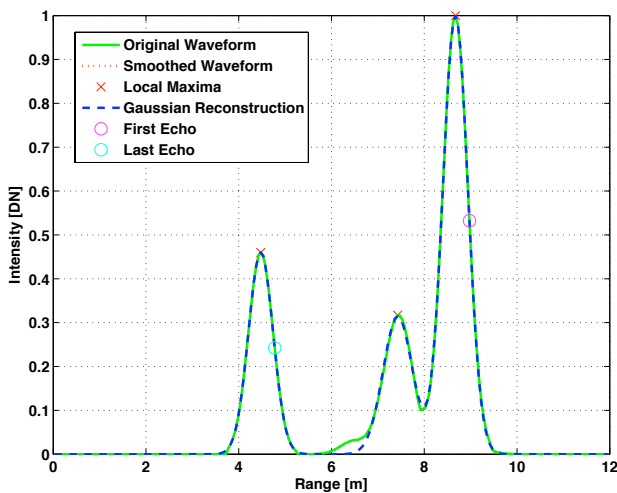

Figure 3: Illustration of Gaussian decomposition for triggering of first and last returns.

In Figure 4 point clouds both from modeled and real data are displayed, the targets consisted of slats of different width and reflectance's. Reflectance values were measured using an ASD field-spec and assigned to the scene description in povray, which as well contained the explicit geometry of the targets. The modeled scene was sampled at exactly the same location as the real data, based on the location of the real echo locations. In order to obtain this modeled echo distribution, we needed to emulate noise in the echo detection process, which will lead to small peaks in the return signal not being detected. We used a simple intensity threshold to eliminate peaks that are to small to be detected. Doing so, we were able to reproduce the *measured* thicknesses of the slats, which is a function of slat width and slat reflectance in conjunction with the characteristics of the detection methodology. We were able to reproduce the effect of target reflectivity of the dark slats in the modeled data. A slat being 5cm wide, and white (third from right in Fig. 4,ρ at 1560 nm : 0.52) will trigger more returns than a black one with a reflectance of only 0.02 (right most in Fig. 4). For more details regarding the experiments on the airstrip, please refer to Wotruba et al. [2005].

2.2 Simulating effects of ALS system specification

Two parameters which are supposed to severely influence ALS return statistics are the footprint size, that is the size of the illu-

minated area on the earth's surface and the different laser wavelengths used in ALS systems. The footprint size depends on beam divergence γ and flight altitude h (and in some cases the aperture D of the transmitter/receiver optics):

$$A = D + 2h \, tan(\frac{\gamma}{2}) \qquad (2)$$

Since D can be neglected in most cases, and γ is generally very small, Equation 2 can be rewritten to:

$$A = h * \gamma \qquad (3)$$

It is known that the size of the footprint alters the ability of the laser pulse to penetrate vegetation [Nilsson, 1996; Chasmer et al., 2006]. The smaller the footprint is, the larger is the chance of not receiving a last echo from the ground in denser vegetation. Thus, for systems recording first and last echo, the penetration of vegetation will in fact be better for systems using larger footprints [Schnadt and Katzenbeisser, 2004]. We will alter the footprint size with the factors of 0.5 and 2, which yields three footprint sizes in total together with the nominal footprint size of the Toposys FALCON II system. The other effect we wanted to study is the effect of using different laser wavelengths. Two commonly used wavelengths are 1064 (e.g. Optech ALTM series) and 1560 nm (e.g. Toposys and Riegl systems), and when one studies spectra of canopy elements, one will find large differences in reflectance for these two wavelengths (see Table 2).

	Reflectance		Transmission	
	1064 nm	1560 nm	1064 nm	1560 nm
Bark	0.172	0.365	0	0
Leaf	0.559	0.217	0.188	0.033
Understory	0.332	0.152	0	0

Table 2: Spectral properties of canopy elements for two laser wavelengths.

How sensitive the return statistics are in respect to laser wavelength is yet not known. Thus, we construct two different pine trees for both 1064 nm and 1560 nm wavelength and sample those in the same way as we did for the footprint diameter analysis. The trees are constructed being *gray scale* as we use for all three of R,G,B the same values of reflectance at the particular wavelength, as they are displayed in Table 2.

2.2.1 Fractal models of tree geometry Fractal models (also known as L-systems) have a long tradition in computer graphics
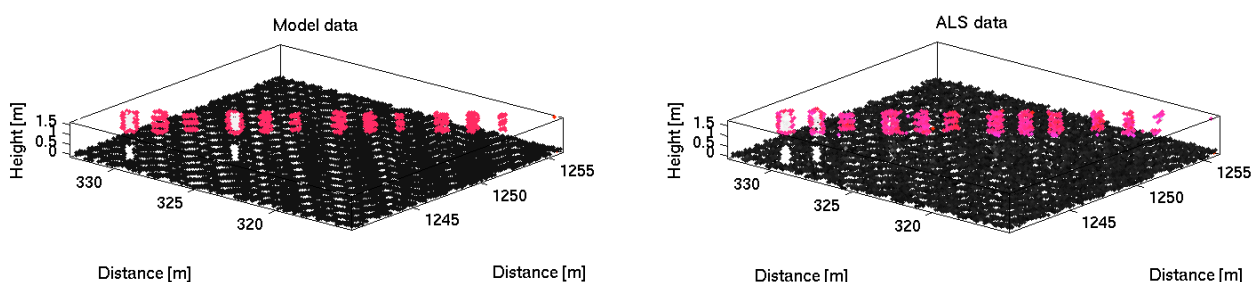
Figure 4: Real ALS data for slats target (right) and modeled data (left). The slats are grouped in 4 colors, with three different widths (15,10 and 5 cm from left to right). The white slats are left, the black ones right. Note the difference in sampled width due to both difference in reflectance and difference in actual width.

Figure 5: Rendered image of modelled pine tree.

for the generation of realistically looking plants. Several Open-Source tools exist which can produce such models for the use in rendering software such as povray. One of these tools, namely Tomtree[3] will be used in this study. A pine tree constructed of the canopy elements leaf and bark is virtually planted on a horizontal patch of soil. These three scene elements (bark,leaf and understory) are assigned with reflectance's and transmissions according to model output of a model for leaf optical properties (PROSPECT, Jacquemoud and Baret [1990]) and ASD field-spec[4] measurements. These values are displayed in Table 2. A side-view rendering of the pine tree used in this study is displayed in Figure 5. The leafs are represented by simple triangles, which are rotated randomly around their elongated axis.

3 RESULTS

3.1 Full waveform

The results for full waveform data are depicted in Fig. 7. The waveforms are averaged from the single simulations and not treated for first and last echo detection as in the previous section, and

---

[3]www.aust-manufaktur.de/austtx.html
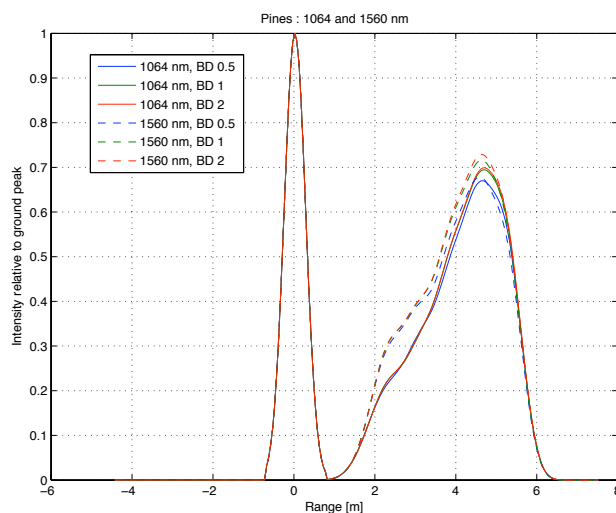[4]www.asdi.com

Figure 7: Averaged waveforms for two wavelengths and three footprint sizes.

thus resemble a height distribution that are being used for e.g. biomass estimation. The different waveforms have been normalized to their ground return, in order to visualize relative differences in the canopy part of the waveforms. We can do this here, since we know that exactly the same area containing the same object has been sampled in our modeling study. In a real world application, normalizing waveforms with the ground peak would not be suitable. For different footprint size, only little (and not significant) differences of about 3 to 5 % in the magnitude of the canopy maximum can be observed. However, for different wavelengths, a significant increase of return energy (about 25 %) below the canopy maximum at about 4.5 m can be observed. The mean energy of the vegetation peak does not significantly change between laser wavelengths of 1064 and 1560 nm. Thus, except for a difference in total energy not shown here (due to normalizing of waveforms), the only significant difference in waveforms is between the 1064 and 1560 nm laser wavelength.

3.2 Discrete returns

In Table 3 the mean height differences of the discrete return statistics for different footprint size are depicted. Bold values indicate that first or last echo distributions are significantly differing from each other based on a two sided Kolmogorov-Smirnow test. First echo statistics are lower on average for large footprint sizes, with this effect being in the order of almost 20 cm, when comparing the returns for 0.5 and 2 mrad beam divergence. For these two
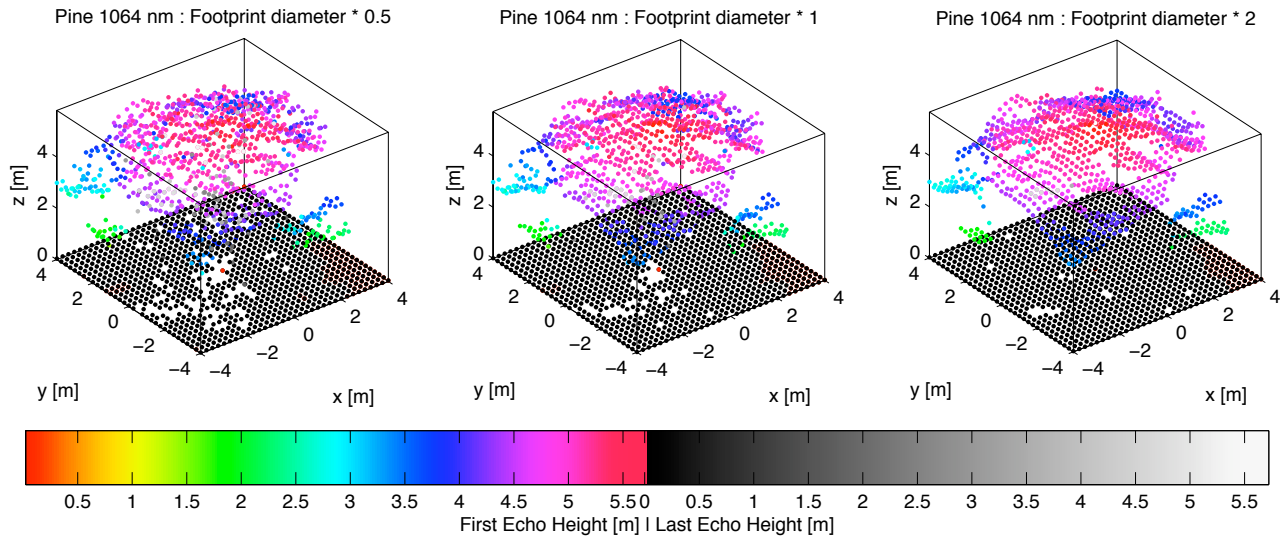
Figure 6: First and last echo distribution inside modelled tree for three different footprint sizes. Note the increased number of ground returns and the smoothing effect due to increase in footprint size.

beam divergences, the difference in first echo distributions is significant. For smaller differences (factor 2) of beam divergence the mean height difference of the first return statistics is not significant. However, last echo distributions are more affected by differences in footprint, as for all three combinations of footprint sizes the distributions are significantly different. Furthermore, a systematic height difference exist when comparing the different footprint sizes. Opposed to first echo statistics, for last echo a positive difference is found when comparing distributions gathered from smaller footprint with those of larger footprints. Thus, one can state that for larger footprint diameters, last echo distribution will be biased upwards. Changing the laser wavelength from 1064 to 1560 nm did not produce significantly different return statistics, neither for first nor for last echo. Thus, these results are not included in Table 3.

Height difference of return statistics [cm]			
Returns Beam diverg. [mrad].	0.5/1	1/2	0.5/2
First echo @ 1064 nm	-10	-6.7	**-17**
First echo @ 1560 nm	-9.6	-5.3	**-15.2**
Last echo @ 1064 nm	**19.3**	**10.1**	**29.5**
Last echo @ 1560 nm	**18.7**	**9.3**	**28.4**

Table 3: Mean height differences in return statistics comparing different footprint diameters. Bold values denote significantly different echo distributions

4 DISCUSSION AND CONCLUSIONS

Using povray and fractal models of tree geometry, we were able to study the effect of two ALS sensor settings on both discrete return statistics and the full return waveform. The model was validated using discrete return data from an experiment on an airstrip, where geometric targets where used to infer information on the effect of target size and reflectance on target visibility. We were able to reproduce the distribution of real data with our model, and could demonstrate that it is sensitive not only for the geometric structure of the modelled objects, but as well for differences in object reflectance. In a sensitivity analysis using a modelled pine tree, we tested the impact of footprint size and laser wavelength on two types of return statistics, discrete return and full waveform. For discrete return data, the return distribution of both first

and last echo do not significantly change in respect to the two laser wavelengths used in this study. For first echo data, the effect of altering footprint size is only significant when changing the footprint diameter by a factor of 4, otherwise the difference of return statistics is not significant. For the last echo statistic, however, even smaller changes in footprint size lead to significantly different return statistics. Furthermore, our results were in conjunction with the statement from Schnadt and Katzenbeisser [2004], showing an increasing number of ground returns when footprint size was increased. First echo distributions will be biased towards the ground, when increasing the footprint size, in the order of some decimeters for our modelled tree. This effect could partly explain the observed increase in tree height underestimation, as was found by Morsdorf et al. [2006a] or Gaveau and Hill [2003], which was in the order of about 30 cm for doubling the flying altitude (and thus the footprint size). Another finding from Morsdorf et al. [2006a] was that there are more last echos triggered inside the canopy for higher flying altitudes. This was said to be related to illumination issues due to the larger footprint, and our modeling results back this behavior to some extent by the observed positive bias in last echo return statistics for larger footprint sizes. In our simulations, first echo data seems to represent an outer hull of the tree crown and does not penetrate deeper into the canopy. This effect was as well observed by Chasmer et al. [2006] in real data, and it might explain why it can be hard to derive canopy density metrics from first echo data alone. For the full waveform, the lower part of the canopy seems to contribute more energy to the return signal at 1560 nm than for 1064 nm laser wavelength. This could be explained by the significantly higher reflectance of leafs at 1064 nm. The canopy elements higher in canopy would already scatter back a large part of the energy of the laser pulse, which in turn would not be available for illuminating the lower part of the canopy.

These forward simulations are a first step in the direction of physically based derivation of biophysical ALS data products and could improve the accuracy of the derived parameters by establishing correction terms for different sensor settings. The model presented in this work can be further used to study the effect of point density, sampling distribution and scanning angle on various canopy types. However, the model might need ecologically calibrated fractal tree models (e.g. AMAP, Castel et al. [2001]) and needs to be validated not only for geometric reference tar-

gets, but as well using real world trees. This will be a difficult task and will most likely be accomplished by incorporating terrestrial laser scanning data. Such modelling will become increasingly important with the availability of small-footprint full waveform data, which needs to interpreted in a meaningful way. If one knows how much ALS system settings contribute to differences in these waveforms, it should be easier to derive accurate descriptions of biophysical parameters from this highly anticipated data, which might provide an even more detailed insight into the vertical structure of vegetation than discrete return data ever could.

5 ACKNOWLEDGMENTS

References

Castel, T., Beaudoin, A., Floury, N., Toan, T. L., Caraglio, Y. and Barczi, J., 2001. Deriving forest canopy parameters for backscatter models using the amap architectural plant model. IEEE Transactions on Geoscience and Remote Sensing 39(3), pp. 571–583.

Chasmer, L., Hopkinson, C. and Treitz, P., 2006. Investigating laser pulse penetration through a conifer canopy by integrating airborne and terrestrial lidar. Canadian Journal of Remote Sensing 32(2), pp. 116–125.

Gaveau, D. and Hill, R., 2003. Quantifying canopy height underestimation by laser pulse penetration in small-footprint airborne laser scanning data. Canadian Journal of Remote Sensing 29, pp. 650–657.

Harding, D., Lefsky, M., Parker, G. and Blair, J., 2001. Laser altimeter canopy height profiles: Methods and validation for closed-canopy, broadleaf forests. Remote Sensing of Environment 76, pp. 283–297.

Hofton, M. A., Minster, J. B. and Blair, J. B., 2000. Decomposition of laser altimeter waveforms. IEEE Transactions on Geoscience and Remote Sensing 38, pp. 1989–1996.

Hyyppä, J., Kelle, O., Lehikoinen, M. and Inkinen, M., 2001. A segmentation-based method to retrieve stem volume estimates from 3-d tree height models produced by laser scanners. IEEE Transactions on Geoscience and Remote Sensing 39, pp. 969–975.

Jacquemoud, S. and Baret, F., 1990. Prospect: A model of leaf optical properties spectra. Remote Sensing of Environment 34(2), pp. 75–91.

Koetz, B., Morsdorf, F., Sun, G., Ranson, K. J., Itten, K. and Allgower, B., 2006. Inversion of a lidar waveform model for forest biophysical parameter estimation. IEEE Geoscience and Remote Sensing Letters 3, pp. 49–53.

Lefsky, M. A., Cohen, W. B., Acker, S. A., Parker, G. G., Spies, T. A. and Harding, D., 1999. Lidar remote sensing of the canopy structure and biophysical properties of douglas-fir western hemlock forests. Remote Sens. Environ. 70, pp. 339–361.

Lovell, J., Jupp, D., Culvenor, D. and Coops, N., 2003. Using airborne and ground-based ranging lidar to measure canopy structure in Australian forests. Canadian Journal of Remote Sensing 29(5), pp. 607–622.

Means, J. E., Acker, S. A., Fitt, B. J., Renslow, M., Emerson, L. and Hendrix, C., 2000. Predicting forest stand characteristics with airborne scanning lidar. Photogrammetric Engineering & Remote Sensing 66(11), pp. 1367–1371.

Morsdorf, F., Frey, O., Meier, E., Itten, K. and Allgöwer, B., 2006a. Assessment on the influence of flying height and scan angle on biophysical vegetation products derived from airborne laser scanning. In: 3d Remote Sensing in Forestry, 14-15. Feb. 2006, Vienna, Austria.

Morsdorf, F., Kotz, B., Meier, E., Itten, K. and Allgower, B., 2006b. Estimation of LAI and fractional cover from small footprint airborne laser scanning data based on gap fraction. Remote Sensing of Environment 104(1), pp. 50–61.

Morsdorf, F., Meier, E., Kötz, B., Itten, K. I., Dobbertin, M. and Allgöwer, B., 2004. Lidar-based geometric reconstruction of boreal type forest stands at single tree level for forest and wildland fire management. Remote Sensing of Environment 3(92), pp. 353–362.

Næsset, E. and Bjerknes, K.-O., 2001. Estimating tree heights and number of stems in young forest stands using airborne laser scanner data. Remote Sensing of Environment 78(3), pp. 328–340.

Ni-Meister, W., Jupp, D. L. B. and Dubayah, R., 2001. Modeling lidar waveforms in heterogeneous and discrete canopies. IEEE Transactions on Geoscience and Remote Sensing 39(9), pp. 1943–1958.

Nilsson, M., 1996. Estimation of tree heights and stand volume using an airborne lidar system. Remote Sensing of Environment 56, pp. 1–7.

Persson, A., Holmgren, J. and Söderman, U., 2002. Detecting and measuring individual trees using an airborne laser scanner. Photogrammetric Engineering & Remote Sensing 68(9), pp. 925–932.

Schnadt, K. and Katzenbeisser, R., 2004. Unique airborne fiber scanner technique for application-oriented lidar products. International Archives of Photogrammetry and Remote Sensing XXXVI - 8/W2, pp. 19–23.

Solenthaler, B., Schäfli, J. and Pajarola, R., 2007. A unified particle model for fluid-solid interactions. Computer Animation and Virtual Worlds 18(1), pp. 69–82.

Sun, G. and Ranson, K., 2000. Modeling lidar returns from forest canopies. IEEE Transactions on Geoscience and Remote Sensing 38(6), pp. 2617–2626.

Wagner, W., Ullrich, A., Ducic, V., Melzer, T. and Studnicka, N., 2006. Gaussian decomposition and calibration of a novel small-footprint full-waveform digitising airborne laser scanner. ISPRS Journal of Photogrammetry and Remote Sensing 60(2), pp. 100–112.

Wotruba, L., Morsdorf, F., Meier, E. and Nüesch, D., 2005. Assessment of sensor characteristics of an airborne laser scanner using geometric reference targets. International Archives of Photogrammetry and Remote Sensing XXXVI(3/W19), pp. 1–6.

Yu, X., Hyyppä, J., Kaartinen, H. and Maltamo, M., 2004. Automatic detection of harvested trees and determination of forest growth using airborne laser scanning. Remote Sensing of Environment 90, pp. 451–462.